

Pixel level optical-transfer-function design based on the surface-wave-interferometry aperture

Guoan Zheng,^{1,*} Yingmin Wang,² and Changhui Yang^{1,2}

¹Department of Electrical Engineering, California Institute of Technology, Pasadena, CA 91125, USA

²Department of Bioengineering, California Institute of Technology, Pasadena, CA 91125, USA

*gazheng@caltech.edu

Abstract: The design of optical transfer function (OTF) is of significant importance for optical information processing in various imaging and vision systems. Typically, OTF design relies on sophisticated bulk optical arrangement in the light path of the optical systems. In this letter, we demonstrate a surface-wave-interferometry aperture (SWIA) that can be directly incorporated onto optical sensors to accomplish OTF design on the pixel level. The whole aperture design is based on the bull's eye structure. It composes of a central hole (diameter of 300 nm) and periodic groove (period of 560 nm) on a 340 nm thick gold layer. We show, with both simulation and experiment, that different types of optical transfer functions (notch, highpass and lowpass filter) can be achieved by manipulating the interference between the direct transmission of the central hole and the surface wave (SW) component induced from the periodic groove. Pixel level OTF design provides a low-cost, ultra robust, highly compact method for numerous applications such as optofluidic microscopy, wavefront detection, darkfield imaging, and computational photography.

©2010 Optical Society of America

OCIS codes: (240.6680) Surface plasmons; (110.4850) Optical transfer functions.

References and links

1. C. Williams, and O. Becklund, *Introduction to the optical transfer function* (SPIE-International Society for Optical Engineering, 2002).
2. J. Goodman, *Introduction to Fourier optics* (Roberts & Company Publishers, 2005).
3. T. Ebbesen, H. Lezec, H. Ghaemi, T. Thio, and P. Wolff, "Extraordinary optical transmission through sub-wavelength hole arrays," *Nature* **391**(6668), 667–669 (1998).
4. T. Thio, K. M. Pellerin, R. A. Linke, H. J. Lezec, and T. W. Ebbesen, "Enhanced light transmission through a single subwavelength aperture," *Opt. Lett.* **26**(24), 1972–1974 (2001).
5. H. J. Lezec, A. Degiron, E. Devaux, R. A. Linke, L. Martin-Moreno, F. J. Garcia-Vidal, and T. W. Ebbesen, "Beaming light from a subwavelength aperture," *Science* **297**(5582), 820–822 (2002).
6. T. Thio, H. Lezec, T. Ebbesen, K. Pellerin, G. Lewen, A. Nahata, and R. Linke, "Giant optical transmission of sub-wavelength apertures: physics and applications," *Nanotechnology* **13**(3), 429–432 (2002).
7. F. J. Garcia-Vidal, L. Martin-Moreno, H. J. Lezec, and T. W. Ebbesen, "Focusing light with a single subwavelength aperture flanked by surface corrugations," *Appl. Phys. Lett.* **83**(22), 4500 (2003).
8. D. Pacifici, H. Lezec, and H. Atwater, "All-optical modulation by plasmonic excitation of CdSe quantum dots," *Nat. Photonics* **1**(7), 402–406 (2007).
9. E. Laux, C. Genet, T. Skauli, and T. Ebbesen, "Plasmonic photon sorters for spectral and polarimetric imaging," *Nat. Photonics* **2**(3), 161–164 (2008).
10. H. Liu, and P. Lalanne, "Microscopic theory of the extraordinary optical transmission," *Nature* **452**(7188), 728–731 (2008).
11. J. O. Tegenfeldt, O. Bakajin, C.-F. Chou, S. S. Chan, R. Austin, W. Fann, L. Liou, E. Chan, T. Duke, and E. C. Cox, "Near-field scanner for moving molecules," *Phys. Rev. Lett.* **86**(7), 1378–1381 (2001).
12. X. Heng, D. Erickson, L. R. Baugh, Z. Yaqoob, P. W. Sternberg, D. Psaltis, and C. Yang, "Optofluidic microscopy--a method for implementing a high resolution optical microscope on a chip," *Lab Chip* **6**(10), 1274–1276 (2006).
13. X. Cui, L. M. Lee, X. Heng, W. Zhong, P. W. Sternberg, D. Psaltis, and C. Yang, "Lensless high-resolution on-chip optofluidic microscopes for *Caenorhabditis elegans* and cell imaging," *Proc. Natl. Acad. Sci. U.S.A.* **105**(31), 10670–10675 (2008).

14. X. Heng, X. Cui, D. W. Knapp, J. Wu, Z. Yaqoob, E. J. McDowell, D. Psaltis, and C. Yang, "Characterization of light collection through a subwavelength aperture from a point source," *Opt. Express* **14**(22), 10410–10425 (2006).
15. S. Maier, *Plasmonics: fundamentals and applications* (Springer Verlag, 2007).
16. H. Lezec, and T. Thio, "Diffracted evanescent wave model for enhanced and suppressed optical transmission through subwavelength hole arrays," *Opt. Express* **12**(16), 3629–3651 (2004).
17. L. Chen, J. T. Robinson, and M. Lipson, "Role of radiation and surface plasmon polaritons in the optical interactions between a nano-slit and a nano-groove on a metal surface," *Opt. Express* **14**(26), 12629–12636 (2006).
18. G. Gay, O. Alloschery, B. Viaris de Lesegno, C. O'Dwyer, J. Weiner, and H. J. Lezec, "The optical response of nanostructured surfaces and the composite diffracted evanescent wave model," *Nat. Phys.* **2**(4), 262–267 (2006).
19. P. Lalanne, and J. Hugonin, "Interaction between optical nano-objects at metallo-dielectric interfaces," *Nat. Phys.* **2**(8), 551–556 (2006).
20. L. Aigouy, P. Lalanne, J. P. Hugonin, G. Julié, V. Mathet, and M. Mortier, "Near-field analysis of surface waves launched at nanoslit apertures," *Phys. Rev. Lett.* **98**(15), 153902 (2007).
21. B. Ung, and Y. Sheng, "Optical surface waves over metallo-dielectric nanostructures: Sommerfeld integrals revisited," *Opt. Express* **16**(12), 9073–9086 (2008).
22. G. Zheng, X. Cui, and C. Yang, "Surface-wave-enabled darkfield aperture for background suppression during weak signal detection," *Proc. Natl. Acad. Sci. U.S.A.* **107**(20), 9043–9048 (2010).
23. E. Palik, and G. Ghosh, *Handbook of optical constants of solids* (Academic press, 1985).
24. J. B. Leen, P. Hansen, Y. T. Cheng, and L. Hesselink, "Improved focused ion beam fabrication of near-field apertures using a silicon nitride membrane," *Opt. Lett.* **33**(23), 2827–2829 (2008).
25. http://www.imagine-optic.com/iop_products_wavefront-analysis-sensors_main_en.php.
26. R. Ng, M. Levoy, M. Bredif, G. Duval, M. Horowitz, and P. Hanrahan, "Light field photography with a hand-held plenoptic camera," *Computer Science Technical Report CSTR 2*, (2005).
27. P. Green, W. Sun, W. Matusik, and F. Durand, "Multi-aperture photography," *ACM Trans. Graph.* **26**(3), 68 (2007).

1. Introduction

Optical transfer function (OTF) characterizes the response of an imaging system as a function of spatial frequency of the input signal. Modification of OTF (sometimes referred as spatial filtering) is of significant importance for modern imaging and vision system designs. The implementation of spatial filtering can be achieved by inserting a mask (phase, amplitude or both phase and amplitude) into the Fourier plane of a 4f system [1], or by using a spatial light modulator (SLM) to modify the phase and amplitude in real time [2]. While these implementation methods allow for good control of OTF, they do come with the associated cost of sophisticated bulk optical arrangement.

In the past years, modulated transmission of subwavelength aperture in metal layer has drawn much attention due to its potential applications from optoelectronics to chemical sensing and biophysics [3–10]. In this letter, we show that the design of OTF can be achieved by modulating the transmission of a bull's eye structure in an ultra compact format. The proposed bull's eye structure makes use of the surface wave interference to modify the spatial response of a conventional circular aperture and we refer it as Surface-Wave-Interferometry Aperture (SWIA). The SWIA can be directly incorporated onto the pixel level of a modern CMOS active pixel sensor (APS) design, creating a new scheme for on chip OTF engineering that are much more compact and robust than those currently achievable options with bulk optical arrangements. In addition, the use of subwavelength aperture for on chip high resolution imaging is of particular interest recently [11–13]. The ability to modify the spatial response of single aperture on pixel level is beneficial to the design of various aperture based imaging devices [14].

2. Principle and simulation

Subwavelength-feature interaction at metallo-dielectric interface involves two kinds of surface waves: the long range surface plasmon (SP) wave and a short range surface scattered wave. SP wave is a electromagnetic surface wave existing at the interface between a dielectric and a noble metal [15]. The SP wave has a wave vector of $k_{sp} = k_0 \sqrt{\epsilon_m \epsilon_d / (\epsilon_m + \epsilon_d)}$, where k_0 is the free space wave vector, and ϵ_m and ϵ_d are the permittivity of the metal and dielectric. In the

past years, SP wave has generated considerable interest thanks to its intrinsic field localization and ability for manipulation of light on the subwavelength scale [15]. Recently, some theoretical and experimental results [10,16–21] also show that a surface scattered component with free space wave vector also plays a role in the short range interaction at the metallo-dielectric interface.

Based on the optical interaction of these surface waves (SW), it has been shown that, single hole surrounded by concentric groove (i.e. the bull's eye structure) can find applications in light enhancement [4,6], beaming [5], spectral imaging [9] and background suppression [22]. Here, we want to demonstrate the capability of the bull's eye structure in modifying the spatial response of the conventional circular aperture. As shown in Fig. 1, an incoming plane wave illuminates at the SWIA with a certain incident angle θ . For a conventional circular hole, only the direct transmission component can be induced; and thus, the spatial response of the transmission follows the cosine function as a first order approximation. For the proposed SWIA in Fig. 1, there are two wave components at the center hole opening: 1) the direct transmission component from the incoming wave; 2) the SW component induced by the concentric groove. By precisely matching the amplitude of the direct light transmission component through the opening with the surface-wave induced component, and arranging the phase shift between the two components to be 180 degrees, we can arrive at a destructive interference condition with no light transmission through the SWIA. Therefore, the spatial response of the center hole opening has been modified due to the SW interference.

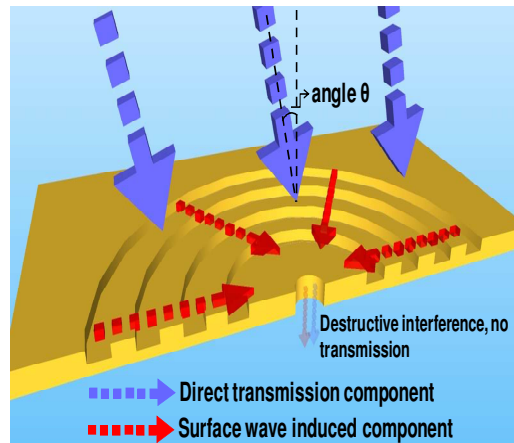


Fig. 1. Working principle of the proposed OTF design scheme. The incoming incident plane wave (with certain transverse wave vector) is coupled into surface waves by the circular groove pattern. The destructive interference between the surface wave component and the direct transmission component results in zero transmission and produces a node in the OTF curve. The principle of OTF design is based on the tuning this destructive interference point by adjusting the spacing between the central hole and inner most groove.

The amplitude matching can be accomplished through judicious choice of central hole size, groove periodicity ('p' in Fig. 2(a)) and the number of grooves. The central hole size is typically chosen to be sufficiently small so that it does not support multi-mode transmission. As the central hole size reaches the multi-mode region, it becomes difficult to satisfy the destructive condition simultaneously for all guided modes in the opening. The periodicity and depth of the groove can be used to control the coupling efficiency of the SW to match direction transmission component. The phase shift is primarily governed by the distance between the central hole and the innermost groove ('s' in Fig. 2(a)). The OTF design principle is based on adjusting the phase difference between the direct transmission and SW induced components. For a highpass OTF design, we adjust the spacing between the central hole and

the inner most grooves such that, the two components in Fig. 1 are 180-degree out of phase under light incidence with low spatial frequency (small incident angles). As such, the two mentioned components will destructively interfere and result in no light transmission in presence of low spatial frequency light incidence (i.e. creating a node at the spatial-response curve). By further altering the 's' spacing, we can move the destructive interference condition further out and create a notch filter and a limited form of low-pass OTF filter.

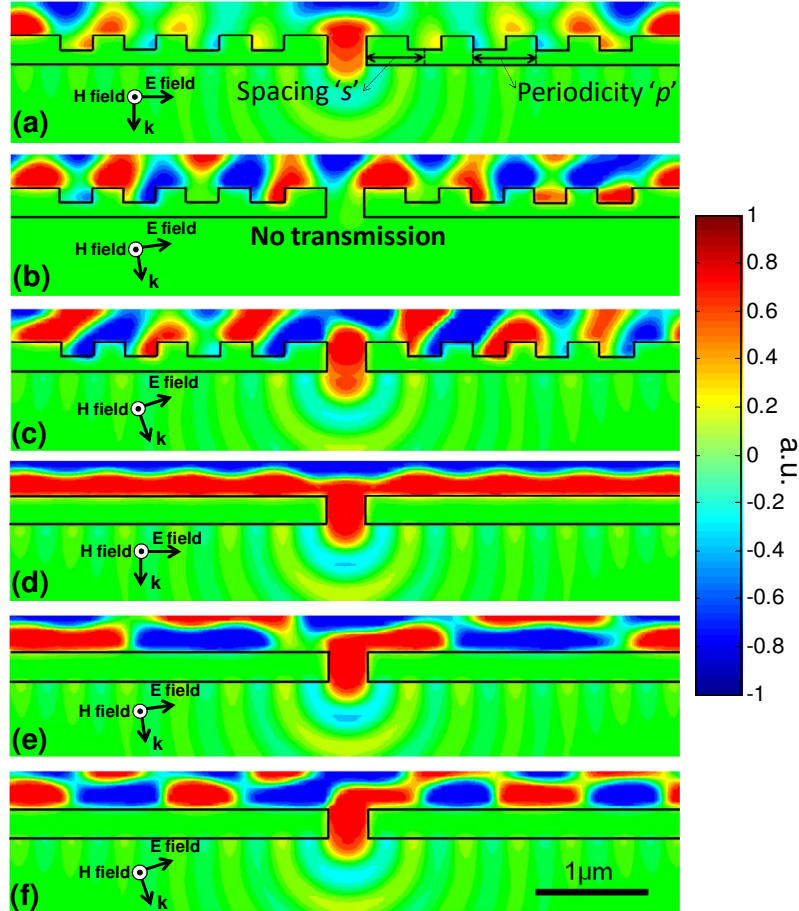


Fig. 2. Simulations results of the OTF notch filter design. Displayed is the real part of the magnetic-field at $\lambda = 740$ nm (equivalent to the time-domain fields at the instant of time when the source phase is zero). (a-c) The simulation of the proposed aperture with 0, 15, and 30 degree incidence. The parameters of the structure are: $s = 540$ nm, $p = 560$ nm, thickness of gold = 340 nm, diameter of hole = 300 nm, groove depth = 140 nm and refractive index of the dielectric substrate = 1.5. (d-f) The simulation of the single hole with 0, 15, and 30 degree incidences.

Figure 2 illustrates a set of simulations of the proposed SWIA. The parameters of these simulations are optimized for a notch OTF design. The simulations are performed by using a commercial software package – CST Microwave Studio. The calculation domain is $12\lambda \times 12\lambda \times 3\lambda$ and contains ~ 12 million meshes. We chose gold as the metal layer based on its low SP loss, good stability and good compatibility with on chip bio applications. The simulations were performed at a nominal wavelength of 740 nm. The permittivity of gold at this wavelength is $-20 + 1.5i$ [23]. The case of single hole is also shown as a reference. As we can see from Fig. 2(a)–2(c), the transmission of the proposed structure quickly dropped to zero at the 15-degree incidence. Since different incident angle corresponds to different spatial

frequency component, the structure in Fig. 2 is a notch OTF filter where the 15-degree incidence component produces a node in the OTF curve. Compared to the case of the single hole without the groove structures, the proposed structure provided a sharp gradient response of the incident angles at the region from 0 to 15 degrees. This unique property of the structure can be used in wavefront detection, where the intensity of the transmission can be mapped to the incident angle of the incoming light field above the aperture. Since the node of the OTF curve can be changed by adjusting the ‘s’ spacing, the design of lowpass and highpass OTF filter can be accomplished by tuning the node to the desired spatial frequency component. We also note that if we change the central hole size of the SWIA without altering the groove structure, the destructive interference won’t be perfect; and thus, there is a residue transmission at the node of the OTF curve.

3. Experiment

We next fabricated a number of the proposed SWIA with different spacing ‘s’ based on the parameters suggested by the simulation results. We used a 1 mm thick glass slide (VWR SuperClean 2 Microarray Substrate) as the substrate for the fabrication. A 2 nm titanium layer was deposited to the substrate as an adhesion layer, and then a 340 nm thick gold layer was coated by using an e-beam evaporator (Temescal BJD-1800). We used focused ion beam (FEI Nova200 dual-beam system using Ga + ions and a 5 nm nominal beam diameter) to mill the hole and the groove structure. A low current beam (30keV, 30pA) was used during the milling process in order to accomplish the requisite fine structure. Figure 3 shows the scanning electron microscope (SEM) image of a typical structure.

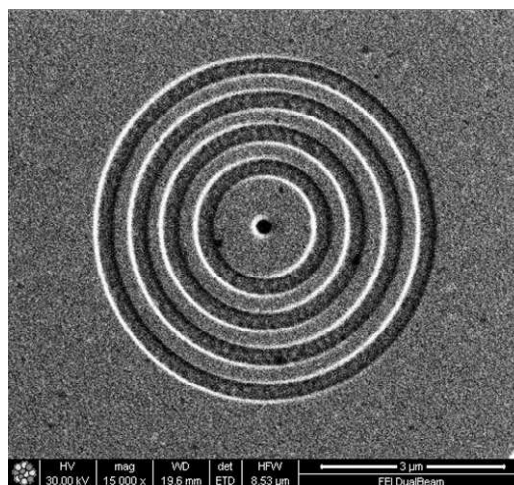


Fig. 3. The SEM image of a typical fabricated aperture.

The experimental set up for characterizing the spatial response of the proposed structure is shown in Fig. 4. We use a Ti-Sapphire laser (Spectra-Physics Tsunami, continuous wave) as the illumination source (wavelength of 740 nm). The transmission of the proposed aperture was collected by a 20X (0.5NA) objective and the whole detection set up was assembled on a motorized rotation stage to measure the spatial response of the aperture with different transverse wave vector of the incident light. The measured data for three different spacing ‘s’ is shown in Fig. 5(a)–5(c), corresponding to notch, highpass and lowpass OTF designs. The case of a single hole is shown in Fig. 5(d) as a reference. We also show the simulation results as a comparison. In the simulation set up, we calculate the transmission of the proposed aperture by integrating the Poynting vector over a $6\lambda \times 6\lambda$ region (0.85λ beneath the aperture). From Fig. 5, we can see that the experiment data are in a good agreement with the simulations, verifying the OTF design scheme of the SWIA. The discrepancy between

measured and simulation data is possibly due to the imperfection of the focus ion beam milling process. To further match these two results, it is possible to anneal the sample to increase the coating quality and using a sacrificial layer to preserve the sharpness of the edge [24].

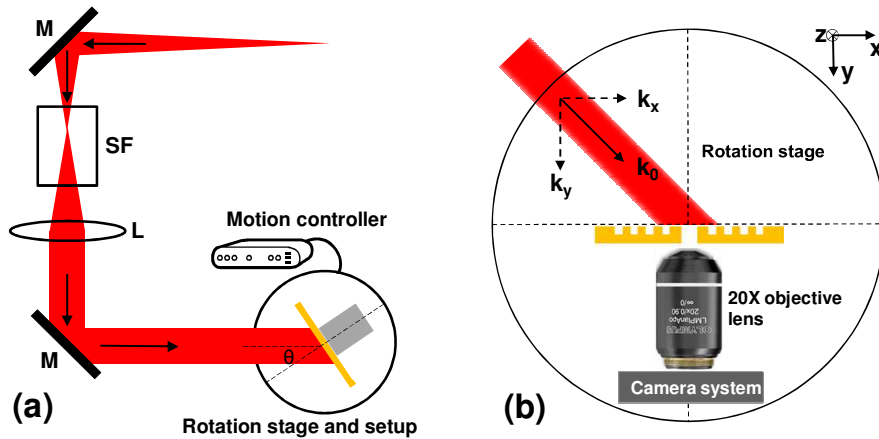


Fig. 4. (a) Illustration of the experimental scheme. A spatially filtered, expanded and collimated laser beam is incident on the aperture in a gold film evaporated on a glass slide. The gold coated glass slide and the light collecting optics are assembled on a rotation stage. M-mirror, SF- spatial filter, L- plano-convex lens. (b) Detailed illustration of setup on the rotation stage.

The different filter designs presented in this paper may find important applications due to the interesting properties they exhibit and the fundamental compactness and cost-effectiveness of their construction. The notch filter profile in Fig. 5(a) shows a very interesting property of the spatial response of the SWIA. The transmission of the SWIA drops from maximum to almost zero from 0 to 15-degree incidence. Compared with the conventional single aperture where the gradient of transmission versus incident angle is always close to zero at normal incidence, the large gradient shown in Fig. 5(a) can be used for wavefront detection. In such a wavefront detection scheme, we should also fabricate a single hole close to (at about $2\mu\text{m}$) the proposed SWIA. As such, the intensity of incoming light does not dramatically change on these two apertures, and we can decompose the wavefront information from the intensity information by the following steps: 1) get the intensity from the single hole; 2) get the intensity from the SWIA and normalized it by the value of the single hole; 3) map this normalized value to a pre measured calibration curve to get the incident angle of the incoming light. Since the proposed SWIA and the single hole aperture can be fabricated directly on top of CCD or CMOS sensor pixels, the whole wavefront detection process can be done on a conventional sensor chip with a high spatial sampling rate (at least two order of magnitude larger than the microlenses array used in a conventional Shack-Hartmann wavefront sensor [25]). The ability to capture the intensity and wavefront information at the same time can also find some application in plenoptic camera, which uses a microlenses array to capture 4D light field information [26].

The high-pass OTF profile shown in Fig. 5(b) can be used in darkfield imaging. The low spatial frequency background illumination will not be transmitted due to the destructive interference. Such an aperture only captures the high frequency components contributed by the object's scattering. We also see that the maximum transmission occurs at the normalized spatial frequency (k_x/k_0) of 0.3. Such a SWIA acts as an optical antenna, with its main lobe of receiving pattern oriented at certain angle. The angle-oriented directivity of the proposed SWIA is equivalent to using a ring aperture in the lens system in multiaperture photography

[27]. With different main lobe orientations, the proposed SWIA can also find some application in depth of field extrapolation and refocusing [27].

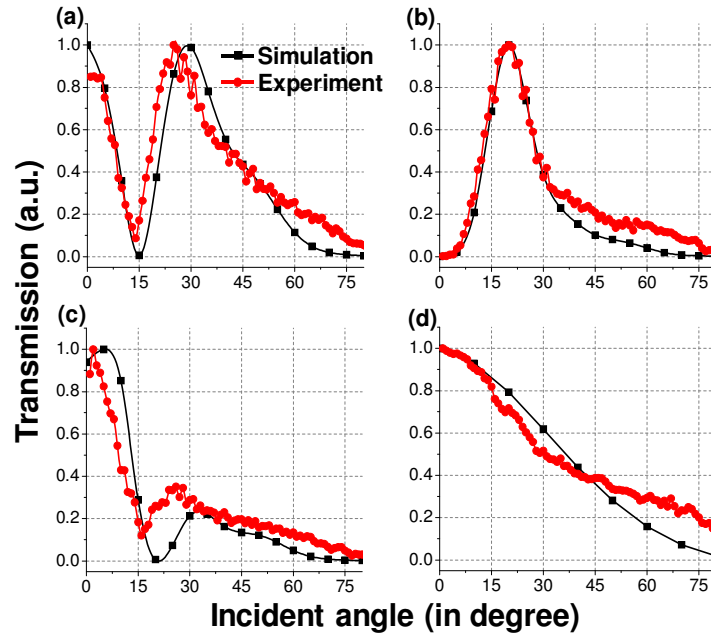


Fig. 5. The spatial response of the proposed aperture. (a - c) the measure and simulated results with different spacing $s = 540$ nm, 780 nm and 460 nm, corresponding to a notch, lowpass and highpass OTF designs. (d) The case of a single hole.

In Fig. 5(c), we show the profile for a limited low-pass OTF structure. The full width at half maximum (FWHM) of the OTF curve is about 20 degrees, only 30% percent of the FWHM of the single hole aperture. The smaller of FWHM curve means the smaller of the collection angle, and thus, a smaller of the f-number of the imaging system and a larger depth of field. In addition, the small value of FWHM is critical for the design of aperture based imaging devices where apertures are used as light collection units [14]. One example is the optofluidic microscope (OFM) [12,13], where the resolution degraded as the height between the sample and the aperture increases. Since the FWHM value of the proposed aperture is only 30% of the conventional single hole, the resolution of the OFM can be increased by $\tan 60^\circ / \tan 20^\circ \approx 5$ folds (provided that it is still in the diffraction limited region).

4. Conclusion

In conclusion, we have demonstrated the OTF design on the pixel level by using SW interference. Three different kind of OTF designs (notch, highpass and lowpass) are shown by adjusting the spacing parameter 's'. Different potential applications such as wavefront detection, optofluidic microscope, wavefront detection, darkfield imaging, computational photography, are discussed. One of the limitations of the proposed OTF design scheme is the requirement of a coherent monochromic light source illumination; however, we believe that such a scheme also works for LED sources as long as the coherent length of the light sources is larger than the proposed aperture size. It is also possible to design broadband SWIA by using more complicated groove structures. This is an area worth further research. Another limitation of the present scheme is the single destructive interference point created by SW and the direct transmission component. From the point view of the conventional analogue filter design, the scheme present in this paper is similar to create a two order transfer function, with one zero at a finite frequency and the other one at the infinite. A more sophisticated method is

to create grooves with different periods; as such, multibeam interference can lead to two or more destructive interference points in OTF curve. Finally, it is worth noting that, while our analysis has thus far been performed with TM wave, SWIA can also work with TM/TE combination or TE wave as well. A detailed study of the proposed SWIA, for example, the role of SP and surface scattered wave, the coupling efficiency of the groove, the phase shift of the SW coupling, the OTF design procedure and its relation to the conventional analogue filter design methods, is highly desired in the future.

Acknowledgements

We are grateful for the constructive discussions with and the generous help from Dr. Jigang Wu and Mr. Lap Man Lee from Caltech. We appreciate the assistance of the Watson cleanroom and Kavli nanoscience institute at Caltech. This work is funded by the Wallace Coulter Foundation, National Science Foundation Career Award BES-0547657, NIH R21EB008867-01.